Conductance of an array of elastic scatterers: A scattering-matrix approach

M. Cahay,* M. McLennan, and S. Datta
School of Electrical Engineering, Purdue University, West Lafayette, Indiana 47907
(Received 16 November 1987)

In the past, the conductance of disordered systems has been extensively studied with use of the Anderson tight-binding Hamiltonian. In this paper we use a different model, which views the semiconductor as regions of free propagation with occasional elastic scattering by a random array of scatterers. Each impurity is characterized by a scattering matrix which can, in principle, be derived for any arbitrary scattering potential. The randomness is introduced through the impurity location. The overall scattering matrix of the device is calculated by combining (using the appropriate law of composition) the scattering matrices of successive sections. The conductance is then evaluated with use of the multichannel Landauer formula. One advantage of this approach is that the quantum conductance can be compared with the semiclassical conductance, which is determined by combining the probability scattering matrices obtained by replacing each element of the (amplitude) scattering matrices by its squared magnitude. This comparison allows us to see clearly the effects of quantum interference. Numerical examples illustrating the onset of weak and strong localization, as well as conductance fluctuations, are presented. Even for samples shorter than the electron elastic mean free path, the size of the conductance fluctuations is close to the universal value if the two-probe conductance formula is used, though it is much larger when the four-probe formula is used.

I. INTRODUCTION

Over the past few years, many experiments on the conductance of disordered metals and semiconductors have been reported in favor of the scaling theory of localization.[1] More recently, the presence of universal conductance fluctuations in disordered systems has been established both experimentally[2-7] and theoretically.[8-13] Such fluctuations have a universal magnitude $\sim e^2/h$ in the weak-localization regime (where $G > e^2/h$) and have been observed by varying the chemical potential in silicon metal-oxide-semiconductor field-effect transistors (MOSFET's),[4,6] and by varying the magnetic field in both metallic samples[2] and $Al_xGa_{1-x}As/GaAs$ heterostructures.[3,5,7] Theoretically, it has also been shown that such conductance fluctuations could occur in metals, due to the motion of a single carrier.[8] The conductance fluctuations arise from a quantum-interference effect which requires phase coherence of the wave functions over large regions of the sample. Most of the theoretical work concerned with the problem of localization and with the size of the conductance fluctuations has been based on the Anderson tight-binding model.[13-15] The results of numerical simulations agree fairly well with the universal value predicted by the perturbative calculations. Another model that has been studied is a purely-one-dimensional (single moded) disordered system, in which the randomness is introduced through the average spacing between impurities (spatial disorder) or through the actual shape of the potential (potential shape disorder).[16-19] In the present paper we generalize this model to allow for multimoded propagation in the disordered material, and we use it to study both localization and conductance fluctuations. The maximum number of propagating modes considered in our numerical examples is 40. This corresponds to the number of propagating modes at the Fermi level in a two-dimensional GaAs resistor [see Fig. 1(a)] with a width of 5×10^3 Å and carrier density of 10^{12} cm^{-2}. Our model is thus well suited to describe the transport properties of realistic semiconductor microstructures such as narrow MOSFET's,[6] GaAs wires,[3] and Aharanov-Bohm structures grown by molecular-beam epitaxy (MBE).[20]

The transport of electrons in a two-dimensional resistor is modeled as regions of free propagation with occasional elastic scattering by a random array of scatterers [see Fig. 1(a)]. We assume the existence of a confining potential in the y direction leading to a set of transverse modes or subbands $m = 1,2,\ldots$ [see Fig. 1(b)] with wave functions of the form

$$\psi_m^{\pm}(x,y)=\phi_m(y)e^{\pm ik_m x}, \tag{1}$$

the $\pm$ signs describing an electron traveling in the positive (negative) x direction, respectively. For simplicity, we assume a parabolic dispersion relation for each mode,

$$E=\varepsilon_m+\frac{\hbar^2k_m^2}{2m^*} \tag{2}$$

ε_m being the energy eigenvalues corresponding to the mth subband.

At zero temperature, the normalized conductance g of the two-dimensional resistor is deduced from the Landauer formula[21,22]

$$g\equiv\frac{G}{e^2/h}=2\sum_{m=1}^{M}\sum_{m'=1}^{M}|t_{m',m}(E=E_F)|^2, \tag{3}$$

where $t_{m',m}$ is the amplitude for an electron injected from

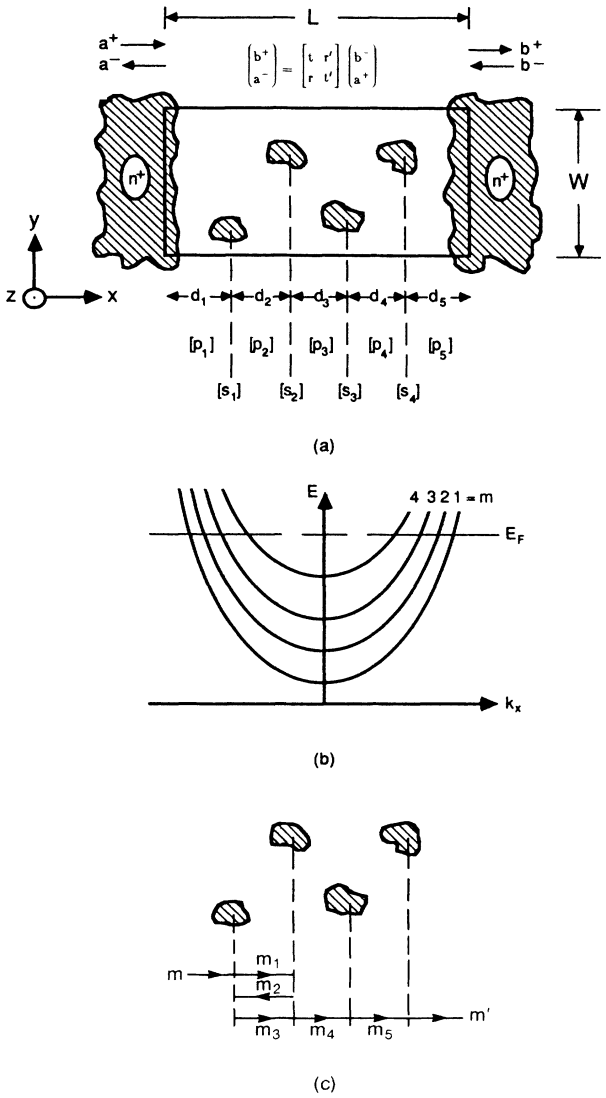

FIG. 1. (a) A two-dimensional resistor. (b) Dispersion relations for different transverse modes. (c) A typical Feynman path from subband m at the left to subband m' at the right.

the left into subband m to be transmitted to subband m' on the right. M is the total number of modes that are occupied at the Fermi level E_F. In previous theoretical work using the tight-binding Hamiltonian, the various transmission coefficients $t_{m',m}$ were calculated using a recursive Green's-function technique.[13,23] Here, we obtain $t_{m',m}$ from the overall scattering matrix of the device, which is calculated by combining (using the appropriate law of composition) the scattering matrices of successive sections.[24–26] In Sec. II we describe the technique used to combine scattering matrices and the two models for impurity scattering that we use in our numerical simulations. We also describe how the semiclassical result (neglecting interference between successive impurities) can be derived from the same formalism simply by combining the probability scattering matrices, obtained by replacing each individual element of the (amplitude) scattering matrices by its squared magnitude.[25] In Sec. III we present the results of a numerical study of the conductance behavior in the weak- and strong-localization regimes using the two models of impurity scattering described in Sec. II. Conductance fluctuations are studied by varying the position of a single impurity out of a large array. The size of the conductance fluctuations is found to be approximately constant in the weak-localization regime, as the number of propagating modes in the sample is changed from 10 to 40. In the strong-localization regime, the size of the fluctuations decreases, as expected. For samples shorter than the elastic mean free path, the size of the fluctuations is close to the universal value if the two-probe formula is used to calculate the conductance; however, fluctuations are much larger if the four-probe formula is used. The main conclusions are summarized in Sec. IV.

II. THEORY

A. Combining scattering matrices

Referring to Fig. 1(a), we wish to calculate the scattering matrix $[s]$ for the resistor, connecting the incoming amplitudes $\{a^+\}$ and $\{b^-\}$ to the outgoing amplitudes $\{b^+\}$ and $\{a^-\}$.

$$\begin{bmatrix} b^+ \\ a^- \end{bmatrix} = \begin{bmatrix} t & r' \\ r & t' \end{bmatrix} \begin{bmatrix} a^+ \\ b^- \end{bmatrix} , \tag{4}$$

where $\{a^\pm\},\{b^\pm\}$ are each $(M\times 1)$ column vectors and $[t]$, $[r]$, $[t']$, and $[r']$ are each $M\times M$ matrices; M is the number of propagating modes available at the Fermi level. The amplitudes are defined so that the probability currents are proportional to their squared magnitudes; conservation of probability then requires that the scattering matrix be unitary. The matrix $[t]$ gives us the M^2 quantities that are needed to evaluate the conductance from Eq. (3). The overall scattering matrix $[s]$ is obtained by combining the scattering matrices of successive sections,

$$[s]=[p_1]\otimes[s_1]\otimes[p_2]\otimes[s_2]\otimes\cdots . \tag{5}$$

$[s_i]$ is the scattering matrix associated with the ith scatterer and $[p_i]$ is the scattering matrix associated with the region of free propagation between the $(i-1)$th and ith scatterer. The symbol $\otimes$ is used to denote combining according to the following law of composition for two scatterers in series.[24–26] If $s_{12}=s_1\otimes s_2$, then

$$t_{12}=t_2[I-r_1'r_2]^{-1}t_1 , \tag{6a}$$

$$r_{12}=r_1+t_1'r_2[I-r_1'r_2]^{-1}t_1 , \tag{6b}$$

$$t_{12}'=t_1'[I+r_2[I-r_1'r_2]^{-1}r_1']t_2' , \tag{6c}$$

$$r_{12}'=r_2'+t_2[I-r_1'r_2]^{-1}r_1't_2' . \tag{6d}$$

We can thus combine $[p_1]$ and $[s_1]$ to get a composite matrix which we then combine with $[p_2]$, and so on until we get the overall matrix $[s]$ of the resistor from Eq. (5). To use Eq. (5) we need the scattering matrices associated

with the individual scatterers and with the regions of free propagation between them. For the latter, since the electrons propagate freely over varying distances $d_1, d_2, \ldots$, the corresponding scattering matrices $[p_1], [p_2], \ldots$ can be written as follows:

$$[p_n] = \begin{bmatrix} \theta_n & 0 \\ 0 & \theta_n \end{bmatrix} . \tag{7}$$

The only nonzero elements are the appropriate phase shifts along the diagonal, i.e.,

$$(\theta_n)_{ij} = e^{ik_j d_n} \delta_{ij} . \tag{8}$$

The problem of calculating the scattering matrix of an individual scatterer is more difficult and will be discussed in Sec. II B.

It will be noted that each of the transmission amplitudes $t_{m',m}$ appearing in the total scattering matrix defined in Eq. (4) is actually the sum over the complex amplitudes $z^{(N)}_{m',m}$ of numerous Feynman paths, originating in subband m at the left and ending in subband m' at the right,

$$T_{m',m} \equiv |\, t_{m',m} \,|^2 = \left| \sum_N z^{(N)}_{m',m} \right|^2 . \tag{9}$$

The superscript N labels the different paths; a typical path is shown in Fig. 1(c). The number of paths is denumerably infinite and we could, in principle, perform the summation in Eq. (9) to calculate $T_{m',m}$, but combining the scattering matrices as described earlier automatically performs this summation for us. In the semiclassical approximation we neglect the interference between scatterers, that is, between the different Feynman paths.

$$(T_{m',m})_{\text{semiclassical}} = \sum_N |\, z^{(N)}_{m',m} \,|^2 . \tag{10}$$

Therefore, the semiclassical T can be calculated in exactly the same way as we calculate the quantum T, except that we combine *probability* scattering matrices $[S_I]$, which are obtained from the amplitude scattering matrices $[s_I]$ by replacing each element by its magnitude squared,[25]

$$[S_I]_{m,n} = |\, [s_I]_{m,n} \,|^2 . \tag{11}$$

Hence the semiclassical scattering matrix $[S_c]$ for the device is given by

$$\begin{aligned} [S_c] &= [P_1] \otimes [S_1] \otimes [P_2] \otimes [S_2] \otimes \cdots \\ &= [S_1] \otimes [S_2] \otimes [S_3] \otimes \cdots , \end{aligned} \tag{12}$$

since it is apparent from Eqs. (7) and (8) that the probability scattering matrices corresponding to free propagation are identity matrices. The semiclassical conductance thus depends only on the number of impurities N_I and is independent of the spacing $d_1, d_2, \ldots$ between the impurities and the wave numbers $k_1, k_2, \ldots$ of the different modes. This is expected, since in the semiclassical approach we neglect any interference between the successive scatterers.

B. S matrix for an individual scatterer

Assuming that the impurity scattering potential $V(\rho)$ is weak, we can write the scattering matrix $[s_I]$ of an individual scatterer using the Born approximation,

$$[s_I] \sim I + i[a] = I + i \begin{bmatrix} a_{++} & a_{+-} \\ a_{-+} & a_{--} \end{bmatrix} , \tag{13}$$

where $[a_{\pm,\pm}]$ are $M \times M$ matrices, and I is the identity matrix of dimension $2M \times 2M$; the matrix elements of $[a_{\pm,\pm}]$ can be shown to be[27]

$$\begin{aligned} (a_{\pm,\pm})_{mn} = & \frac{m^*}{\hbar^2} \frac{1}{[k_m k_n]^{1/2}} \\ & \times \int dx \int dy \, \psi^{\pm *}_m(\rho) V(\rho) \psi^{\pm}_n(\rho) , \end{aligned} \tag{14}$$

where $\psi^{\pm}_m(\rho)$ is the wave function of an electron in subband m with energy E traveling in the positive $(+)$ or negative $(-)$ x direction, and k_m is the x component of the wave vector [Eq. (2)]. The integration in Eq. (14) extends over the region where the impurity potential is nonzero. If γ is the parameter characterizing the strength of the interaction $V(\rho)$, the scattering matrix in Eq. (13) is only unitary to order γ. In order to make it exactly unitary (as it should be), one could use the following ansatz:

$$[s_I] = e^{i[a]} . \tag{15}$$

Indeed, since $[a]$ is Hermitian, $e^{i[a]}$ is exactly unitary. Furthermore, to lowest order in γ, the expression in Eq. (15) agrees with Eq. (13). For our numerical simulations, we have used two different models of impurity scattering based on two different choices for the matrix $[a]$. These are described below.

Model A: In the first model, we assume that each impurity has the same scattering matrix $[s_I]$ given by Eq. (15), where $[a]$ is a Hermitian matrix with all its elements equal:

$$[a]_{m,n} = \alpha \quad \text{for } m,n = 1,2,\ldots,2M . \tag{16}$$

The exponentiation appearing in Eq. (15) can then be performed analytically. One obtains[28]

$$[s_I] = I + \left[\frac{\beta}{\alpha} \right] [a] , \tag{17}$$

where

$$\beta = \frac{e^{2iM\alpha} - 1}{2M} . \tag{18}$$

Thus our choice of scattering matrix implies that at each impurity the incident mode is reflected equally into each of M modes with probability $|\beta|^2$; it is also transmitted equally into each of the other $M-1$ modes with probability $|\beta|^2$. One advantage of this model is that the semiclassical conductance of a sample containing N_I impurities can be calculated exactly using Eqs. (3) and (12) (see Appendix A),

$$g_c = \frac{2M\Lambda_{el}}{\Lambda_{el}+N_I} , \tag{19}$$

where Λ_{el} is the dimensionless elastic mean free path,

$$\Lambda_{el}=(1-M\,|\beta|^2)/M\,|\beta|^2 . \tag{20}$$

It is thus evident that the semiclassical conductance for this model obeys Ohm's law: The resistance g_c^{-1} increases linearly with N_I (or sample length). For $N_I=0$, the resistance is nonzero ($=1/2M$), which can be viewed as the constant resistance.

Model B: Here we assume that each impurity has a δ-function scattering potential given by

$$V(\rho)=\gamma\delta(x-x_i)\delta(y-y_i) , \tag{21}$$

(x_i,y_i) being the position of the ith impurity. The scattering matrix across the δ impurity can be calculated according to the general procedure described above, i.e., using Eqs. (14) and (15). However, for this special case, we do not need the ansatz in Eq. (15); the scattering matrix can be derived exactly (see Appendix B):

$$[s]=\begin{bmatrix} [I+ia_{++}]^{-1} & -[I+ia_{++}]^{-1}(ia_{++}) \\ -[I+ia_{++}]^{-1}(ia_{++}) & [I+ia_{++}]^{-1} \end{bmatrix} , \tag{22}$$

where a_{++} is an $M\times M$ matrix with matrix elements

$$(a_{++})_{mn}=\frac{\tilde{\Gamma}_{mn}}{2(k_m k_n)^{1/2}} , \tag{23}$$

and the coupling parameters $\tilde{\Gamma}_{mn}$ are given by

$$\tilde{\Gamma}_{mn}=\frac{2m^*\gamma}{\hbar^2}\phi_m^*(y_i)\phi_n(y_i) . \tag{24}$$

We can see from Eq. (24) that, unlike model A, the scattering matrix depends on the y location of the scatterer giving rise to an additional degree of randomization in model B. In model B even the semiclassical conductance [Eq. (12)] changes with impurity configuration.

In the next section we will mainly use model A to study localization and universal conductance fluctuations due to the motion of a single impurity in disordered samples. Numerical results using model B are also presented showing the influence of the y location of the impurities on the conductance of two-dimensional (2D) resistors.

III. NUMERICAL EXAMPLES

A. Model A

Figure 2 shows the resistance (g^{-1}) of two samples ($M=30$, $\Lambda_{el}=33.33$) as a function of the number of impurities N_I; the two samples differ in their impurity configuration, which is chosen at random. The distances d_n were distributed uniformly over some range such that $k_i d_n$ ($i=1,2,\ldots,M$) vary between 50π and 250π. Also shown for comparison is the semiclassical result (g_c^{-1}), which is independent of the impurity configuration [Eq. (19)]. The weak- and strong-localization regions are evident. The localization length is defined as the length for which the reduced quantum conductance is about unity, and is given approximately by the following relation:[29]

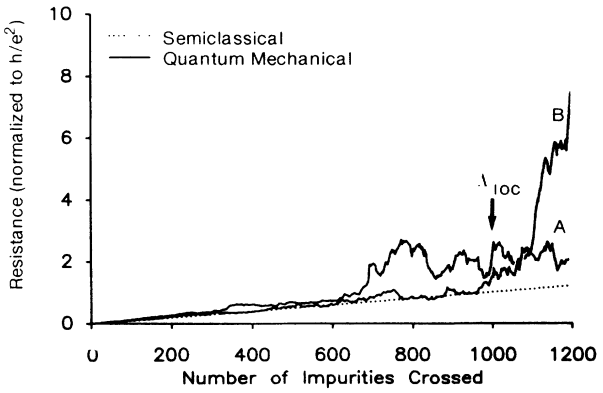

FIG. 2. Normalized quantum-mechanical resistance for two different samples (labeled A and B) vs number of impurities, N_I (model A: $M=30$, $\Lambda_{el}=33.33$). The straight line represents the semiclassical result deduced from Eq. (19) in the text.

$$\Lambda_{loc}=M\Lambda_{el} . \tag{25}$$

To study the fluctuations in the conductance, it is necessary to calculate g for samples with a fixed number of impurities, but with totally different impurity configurations. However, it has been shown that moving a single impurity leads to conductance fluctuations of the same size.[8] Since this is much less time consuming numerically, we calculated the quantum-mechanical conductance g for different samples ($M=30$, $\Lambda_{el}=33.33$) with fixed number of impurities N_I, but with the middle impurity moved by varying distances d such that $k_1 d$ for the lowest mode changed from zero to 200π. It is evident from Fig. 3 that the conductance is uncorrelated when $k_1 d$ is changed by $\sim\pi$. It will be noted that the average conductance is less than the semiclassical conductance by ~ 1. We have checked this for samples with different numbers of impurities, and we find that the quantum con-

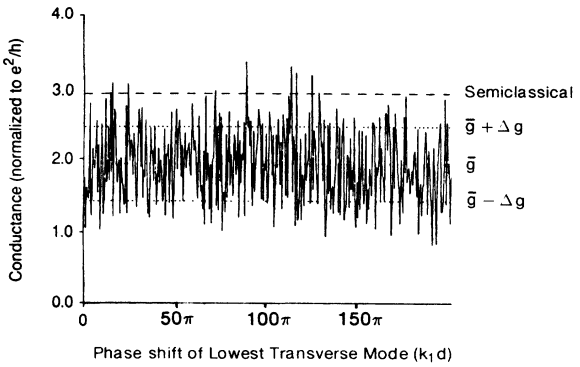

FIG. 3. Universal conductance fluctuations (in a sample containing 600 impurities) due to the motion of the middle impurity a distance d to the right from its original position ($M=30$, $\Lambda_{el}=33.33$). The semiclassical conductance is also shown for comparison.

ductance is consistently smaller than the semiclassical conductance. We believe this to be due to coherent backscattering,[30] so that the reflection probability R_{ii} into the incident mode is enhanced over those into the other modes R_{ij}, as shown in Fig. 4.

In Fig. 3 we notice the large conductance fluctuations whose variance $0.52e^2/h$ is in close agreement with the universal value calculated by diagrammatic techniques.[9] This variance was calculated for samples with different numbers of impurities. As seen in Fig. 5, the size of the conductance fluctuations is approximately constant over the weak-localization regime and gradually decreases below its universal value in the strong-localization regime. This is in agreement with the numerical simulations performed on an Anderson tight-binding Hamiltonian.[13,15]

Figure 6 shows that the size of the conductance fluctuations stays approximately constant ($\sim 0.5e^2/h$) when the number of propagating modes is increased. All the samples considered in this simulation contain a number of impurities, N_I, equal to half the (dimensionless) localization length ($N_I = M\Lambda_{el}/2$). They are all characterized by the same value of the parameter α entering the impurity scattering matrix (17), so that the mean free path Λ_{el} is different for different values of M (Fig. 6). Lee showed that the ratio $\Delta g/g$ should decrease as $\sim 1/M$ if the transmission coefficients $T_{m',m}$ were uncorrelated random variables;[12] the numerical results show that $\Delta g/g$ is nearly constant independent of M, indicating that the coefficients $T_{m',m}$ are correlated.

In the ballistic regime, i.e., for $L < \Lambda_{el}$, the conductance fluctuations were also calculated using the two-probe Landauer formula (3). However, recent experiments performed on metallic rings have employed a four-probe measuring configuration to measure the size of the conductance fluctuations in the presence of an external magnetic field. It has been suggested that a more appropriate Landauer formula to describe these measurements is given by[31,32]

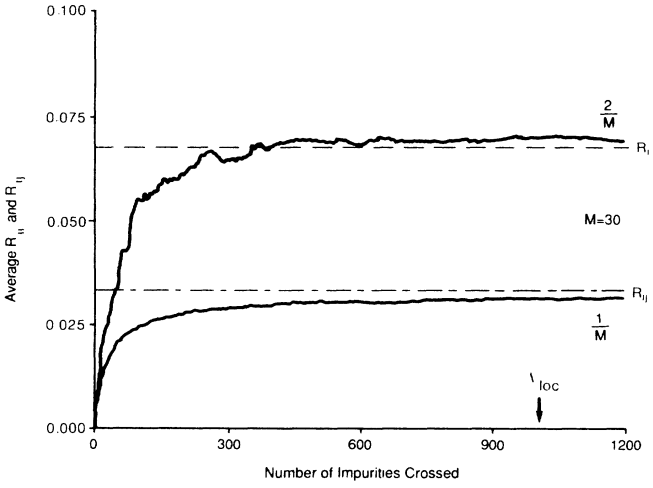

FIG. 4. Average diagonal and off-diagonal reflection coefficients for a specific sample with $M=30$, $\Lambda_{el}=33.33$.

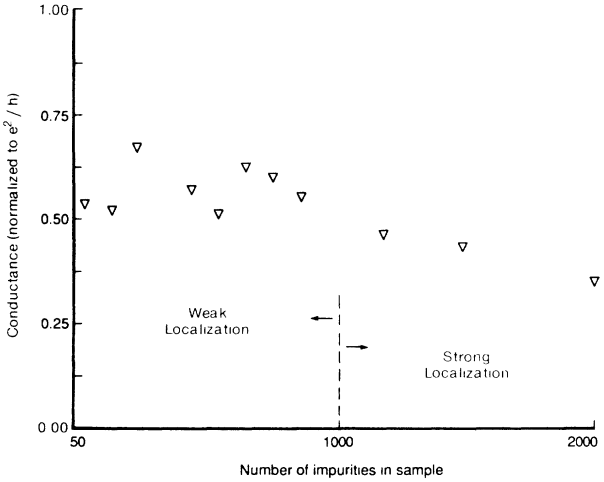

FIG. 5. Variance of the universal conductance fluctuations (due to the motion of the middle impurity) for different sample lengths from weak to strong localization ($M=30$, $\Lambda_{el}=33.33$).

$$g = 2\sum_{m=1}^{M} \frac{T_m}{R_m} , \tag{26}$$

where T_m and R_m are the total transmission and reflection probabilities into the mth mode, i.e.,

$$T_m = \sum_{m'} T_{m,m'} \quad \text{and} \quad R_m = \sum_{m'} R_{m,m'} . \tag{27}$$

Since it is in the ballistic regime that Eqs. (3) and (26) give very different results, we have calculated the size of the conductance fluctuations in this regime using both Eqs. (3) and (26) (Fig. 7). The conductance fluctuations obtained using Eq. (3) decrease slightly below the universal result in the ballistic regime (we expect $\Delta g=0$ for samples containing a single impurity). This agrees with the results obtained using a tight-binding Hamiltonian,[15] for which the universality of the conductance fluctuations was found to be quite robust and valid even for very short samples. On the other hand, the value of Δg obtained from Eq. (26) increases rapidly as the sample length is decreased.

The theoretical predictions concerning the universality of the conductance fluctuations have been deduced from perturbation theory[9,10] to lowest order in $(k_F\Lambda_{el})^{-1}$, where k_F is the Fermi wave vector and Λ_{el} is the elastic mean free path. In all our numerical calculations, too, $k_F\Lambda_{el} \gg 1$, since the average spacing $\{d_n\}$ between impurities was chosen such that $k_F d_n \simeq 50\pi$ for the mode with the highest transverse energy. We find that in model A failure to meet the requirement that $k_F d_n \gg 1$ can introduce spurious results, since there is no other source of randomization. In fact, if we set the average spacing between scatterers, d_n, to zero, each scattering matrix for the free propagation between impurities reduces to

$$[p] = \begin{bmatrix} I & 0 \\ 0 & I \end{bmatrix} . \tag{28}$$

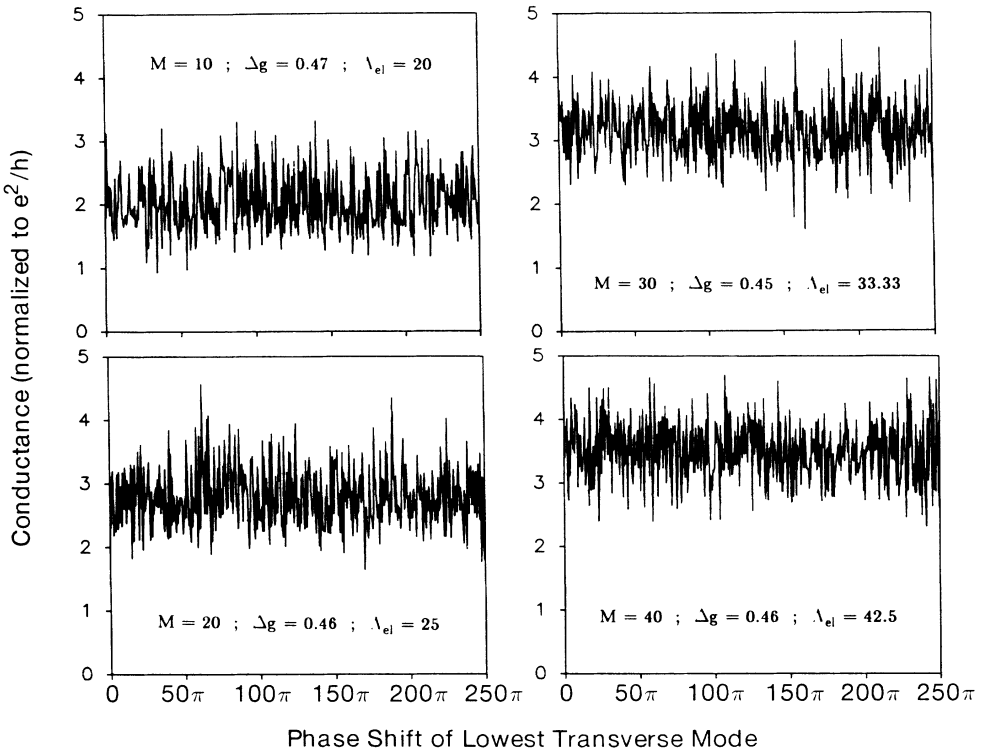

FIG. 6. Conductance fluctuations due to displacement of the middle impurity for different numbers of propagating modes. The number of impurities, N_I, was chosen equal to $M\Lambda_{el}/2$ so that the semiclassical conductance is equal to $2M(1+0.5M)$.

Physically, this means that all the phases of the different modes are small and not fully randomized over 2π between scatterers. In that case, the scattering matrices $[p]$ can be neglected when combining the scattering matrices. We must then combine the scattering matrix $[s_I]$ [in Eq. (17)] with itself a number of times equal to N_I. This can be done analytically. As the number of impurities in the sample goes to infinity, the conductance can then be shown to converge to the following limit,

$$g \rightarrow 2(M-1) , \tag{29}$$

independent of the constant α in Eq. (17). This is a spurious effect arising from the special form of s_I in model A and it goes away as the average spacing between impurities is increased.

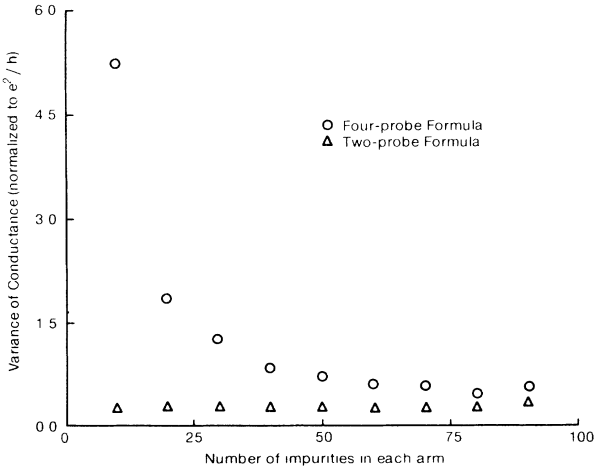

FIG. 7. Conductance fluctuations (due to the motion of a single impurity) calculated using a two-probe [Eq. (3)] and a four-probe [Eq. (26)] conductance formula ($M=30$, $\Lambda_{el}=33.33$).

B. Model B

The resistance versus length of a two-dimensional (2D) resistor (GaAs) with $n_s = 10^{11}$ cm^{-2} was calculated for samples of width 2×10^3 Å ($M=15$). Figure 8 shows a typical sample 2×10^3 Å wide and 2×10^4 Å long, in which the positions of the δ scatterers are chosen randomly with a uniform distribution in both x and y directions for a given impurity concentration. The scattering matrix elements were calculated from Eq. (24) using the eigenfunctions $\phi_m(y)$ appropriate for a particle-in-a-box type of confinement in the y direction. The strength of scattering from a single impurity was chosen so that $\Lambda_{el}\sim400$.[33] Figure 9 shows the quantum resistance calculated for two samples with different impurity configurations. For comparison, the semiclassical resistance was also calculated for the same samples using the technique of combining probability scattering matrices, as described in Sec. II A. It is evident that the quantum-

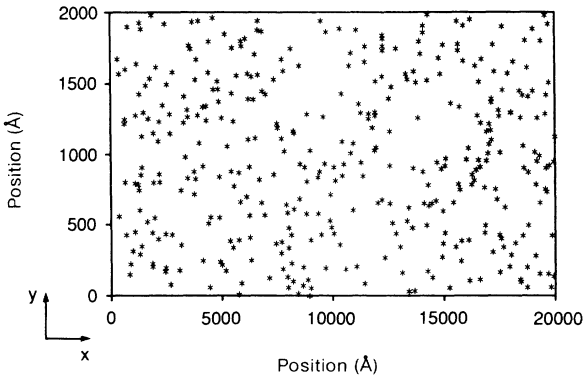

FIG. 8. Model B: A specific sample 2×10^4 Å long and 2×10^3 Å wide. The impurity concentration is 10^{11} cm^{-2}.

mechanical resistance depends strongly on the impurity configuration. Actually, the semiclassical resistances are also slightly different for different samples. This is because, unlike model A, the scattering matrix of an individual scatterer depends on its y location. We expect the variation of the semiclassical resistance from sample to sample (with a fixed number of impurities) to get smaller for wider samples. Quantum mechanically, however, the universal conductance result predicts that the conductance fluctuations for different samples should be of the order of e^2/h, regardless of the width of the samples. Obtaining the variance of the conductance fluctuations over a statistically meaningful number of completely different samples is quite time consuming. However, since conductance fluctuations of the same magnitude can be obtained by the motion of a single impurity,[8] we calculated (both semiclassically and quantum mechanically) the variance of the conductance fluctuations by changing the y position of the middle impurity only from one side of the resistor to the other in steps of 10 Å (Fig. 10). The quantum-mechanical fluctuations are seen to be

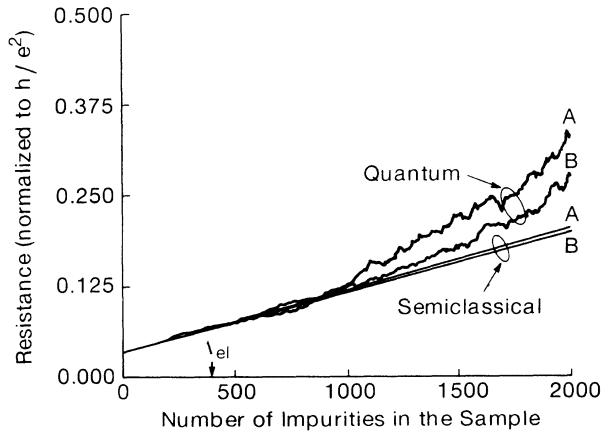

FIG. 9. Resistance vs length for two different samples such as the one shown in Fig. 8 differing by their impurity configuration (the samples are 2×10^3 Å wide). The straight lines represent the semiclassical results ($M=15$, $\Lambda_{el}\sim400$).

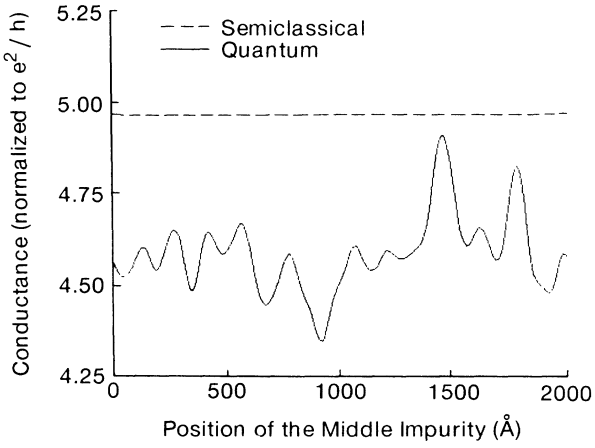

FIG. 10. Semiclassical and quantum-mechanical conductance of a sample such as the one shown in Fig. 8 after moving the middle impurity from one side of the resistor to the other (the x position of the impurity is unchanged). The sample contains 2×10^3 impurities ($M=15$, $\Lambda_{el}\sim400$).

quite large ($\Delta G\simeq0.2e^2/h$), whereas no sensible fluctuation is perceptible in the classical case.

IV. CONCLUSIONS

We have studied the problem of localization and conductance fluctuations in a random array of elastic scatterers, neglecting any inelastic scattering. The overall scattering matrix of the device is calculated by combining the scattering matrices associated with the individual scatterers, and with the regions of free propagation between them. One advantage of combining scattering matrices is that the semiclassical conductance can be derived simply by replacing all amplitude scattering matrices by probability scattering matrices; this allows us to see clearly the effects of quantum interference.

Numerical results for the length dependence of the conductance are in agreement with the scaling theory of localization. In the weak-localization regime, the quantum-mechanical conductance (after averaging over many samples) is shown to be consistently smaller than the semiclassical result. Furthermore, for samples longer than the localization length, the quantum resistance is found to increase exponentially. We investigated the conductance fluctuations due to the motion of a single impurity out of a large array. For sample lengths in the weak-localization regime (i.e., $\Lambda_{el}<L<\Lambda_{loc}$), the size of the conductance fluctuations agrees fairly well with the theoretical universal value for quasi-one-dimensional systems, i.e., $0.53e^2/h$; the size of the fluctuations is found to decrease in the strong-localization regime. In the ballistic regime, the conductance fluctuations are found to be much larger than e^2/h if we use a four-probe formula; with a two-probe formula the conductance fluctuations are close to the universal result. In the weak-localization regime the conductance fluctuations are found to be independent of the number of propagating

modes M in the sample ($10 < M < 40$). Therefore, our simulations support the recent qualitative arguments showing that the various transmission coefficients are correlated random variables. Finally, we have shown that even the semiclassical conductance can vary slightly from sample to sample. This is because the individual impurity scattering matrix depends on the exact location of the impurity as a result of the confining potential perpendicular to the direction of propagation of the current.

One important feature of our model is that it can, in principle, be applied to any arbitrary scattering potential with finite range; it can thus be used in modeling realistic semiconductor microstructures. Recently, various groups have reported the observation of universal conductance fluctuations in ultrasmall GaAs wires and in Aharanov-Bohm heterostructures. In these devices, the spatial quantization reduces the number of propagating channels available at the Fermi level to be of the order of a few tens, which is quite tractable numerically.

ACKNOWLEDGMENTS

This work was supported by the U.S. National Science Foundation under Grant No. ECS-83-51-036 and by the Semiconductor Research Corporation under Contract No. 87-SJ-089.

APPENDIX A: OHM'S LAW

In Sec. II A, we argued that the semiclassical conductance of a random array of scatterers could be deduced by combining probability scattering matrices rather than amplitude scattering matrices. In this appendix, we prove for model A that this leads to Ohm's law for the conductance of a random array of scatterers [Eq. (19)].

Let us consider a random array of scatterers, all characterized by the same scattering matrix [see Eq. (17) in the text]. Using the prescription in Eq. (11), the probability scattering matrix for each scatterer is written as

$$[S_I]=\begin{bmatrix} T & R \\ R & T \end{bmatrix}, \tag{A1}$$

where

$$[R]=\begin{bmatrix} \delta & \cdots & \delta \\ \vdots & & \vdots \\ \delta & \cdots & \delta \end{bmatrix},$$

$$[T]=\begin{bmatrix} 1-(2M-1)\delta & \cdots & \delta & \delta \\ \delta & & \delta & \delta \\ \vdots & & \vdots & \vdots \\ \delta & \cdots & \delta & 1-(2M-1)\delta \end{bmatrix}, \tag{A2}$$

where

$$\delta=|\beta|^2=\left|\frac{e^{2iM\alpha}-1}{2M}\right|^2. \tag{A3}$$

For free propagation between the scatterers, the probability scattering matrix is given by [see Eqs. (7) and (8)]

$$[P_n]=\begin{bmatrix} I & 0 \\ 0 & I \end{bmatrix}. \tag{A4}$$

Now we combine the probability scattering matrices in the same way as the amplitude scattering matrices. It is apparent from Eqs. (6a)–(6d) in the text that $[P_n]$ combined with any matrix $[S_I]$ yields back $[S_I]$. In other words, the lengths $\{d_n\}$ will not appear in the final expression for the semiclassical conductance. Therefore, considering a sample of N_I impurities, the overall scattering matrix is obtained by combining N_I identical scattering matrices $[S_i]$. Consider first the result of combining two sections,

$$[R_2]=[R]+[T][R](I-[R]^2)^{-1}[T]. \tag{A5a}$$

We can write $[R]$ and $[T]$ as

$$[R]=\delta[u], \tag{A5b}$$

$$[T]=(1-2M\delta)I+\delta[u], \tag{A5c}$$

where

$$[u]=\begin{bmatrix} 1 & \cdots & 1 \\ \vdots & & \vdots \\ 1 & \cdots & 1 \end{bmatrix}. \tag{A5d}$$

Equation (A5a) is simplified to yield

$$[R_2]=[R]+\left[\frac{1}{1-M^2\delta^2}\right][T][R][T]. \tag{A6}$$

Here we have used the relation

$$[u]^2=M[u]. \tag{A7}$$

Equation (A6) can be simplified further using Eqs. (A5a)–(A5d) and Eq. (A7),

$$\begin{aligned}[T][R][T]&=[T](1-M\delta)[R] \\ &=(1-M\delta)^2[R].\end{aligned} \tag{A8}$$

Hence,

$$[R_2]=\frac{2}{1+M\delta}[R]. \tag{A9}$$

Thus $[R_2]$ can be written as

$$[R_2]=\delta_2[u], \tag{A10}$$

where

$$\delta_2=\frac{2\delta}{1+\delta}. \tag{A11}$$

Note that

$$\frac{M\delta_2}{1-M\delta_2}=2\left[\frac{M\delta}{1-M\delta}\right]. \tag{A12}$$

Similarly, by combining two sections, each having two scatterers, we can show that

$$[R_4]=\delta_4[u], \tag{A13}$$

where

$$\frac{M\delta_4}{1-M\delta_4}=2\frac{M\delta_2}{1-M\delta_2}=4\frac{M\delta}{1-M\delta} . \tag{A14}$$

We can continue this process indefinitely to get

$$[R_{N_I}]=\delta_{N_I}[u] , \tag{A15}$$

where

$$\frac{M\delta_{N_I}}{1-M\delta_{N_I}}=N_I\left[\frac{M\delta}{1-M\delta}\right] . \tag{A16}$$

Equations (A15) and (A16) are, in fact, valid for all N_I, as can be shown by induction. The conductance g_c of a sample containing N_I impurities is obtained from Eq. (3) in the text,

$$g_c=2M(1-M\delta_{N_I})$$

$$=2M\left[\frac{1-M\delta}{1+(N_I-1)M\delta}\right] , \tag{A17}$$

which can be rewritten as

$$g_c=2M\frac{\Lambda_{\rm el}}{\Lambda_{\rm el}+N_I} \tag{A18}$$

by introducing the elastic mean free path

$$\Lambda_{\rm el}=\frac{1-M\delta}{M\delta} . \tag{A19}$$

This proves Eq. (19) in the text.

APPENDIX B: SCATTERING MATRIX FOR A δ IMPURITY

In this appendix we derive the exact analytical form of the scattering matrix across a δ impurity. Our starting point is the one-electron, effective-mass, time-independent Schrödinger equation,

$$\left[-\frac{\hbar^2}{2m^*}\left[\frac{\partial^2}{\partial x^2}+\frac{\partial^2}{\partial y^2}\right]+E_c(x,y)+V(\boldsymbol{\rho})\right]\Phi(\boldsymbol{\rho})=E\Phi(\boldsymbol{\rho}) , \tag{B1}$$

written for an electron propagating through a two-dimensional device with arbitrary conduction-band–energy profile $E_c(x,y)$ (x being the direction of propagation of the current and y being the direction of confinement of the two-dimensional resistor). In Eq. (B1), $V(\boldsymbol{\rho})$ is the scattering part of the Hamiltonian due to the presence of impurities in the sample (the following derivation is readily extended to 3D structures). For elastic scattering, the electron total energy is conserved while traversing the device. If V is identically equal to zero, the band-energy profile (or external potential energy) is assumed to be separable, i.e.,

$$E_c(x,y)=E_c^x(x)+E_c^y(y) . \tag{B2}$$

The eigenfunctions $\phi_m(y)$ and the eigenvalues ε_m of the y-dependent part of the Hamiltonian can, in principle, be calculated from the equation

$$\left[-\frac{\hbar^2}{2m^*}\frac{\partial^2}{\partial y^2}+E_c^y(y)\right]\phi_m(y)=\varepsilon_m\phi_m(y) . \tag{B3}$$

The (normalized) functions $\phi_m(y)$ form a complete set of eigenstates which can be used to write the general solution of Eq. (B1) in the form

$$\Phi(\boldsymbol{\rho})=\sum_{n=1}^{M}C_n(x)\phi_n(y) . \tag{B4}$$

We limit the summation to include only the M propagating modes. Using Eq. (B4) and making use of the orthonormality of the functions ϕ_m, the Schrödinger equation (B1) can be written as

$$\frac{d^2C_n}{dx^2}+k_n^2(x)C_n=\sum_{m=1}^{M}\Gamma_{nm}(x)C_m , \tag{B5}$$

where

$$k_n^2(x)=\frac{2m^*}{\hbar^2}[E-\varepsilon_n-E_c^x(x)] \tag{B6}$$

and

$$\Gamma_{nm}(x)=\frac{2m^*}{\hbar^2}\int dy\,\phi_n^*(y)V(\boldsymbol{\rho})\phi_m(y) . \tag{B7}$$

Equation (B5) is our main result. The problem of solving the scattering problem is then reduced to the calculation of the coefficients $\Gamma_{nm}(x)$ and to the solution of the system of M coupled differential equations (B5).

In general, both the k_n^2's and the Γ_{nm}'s are functions of the variable x, and depend, respectively, on the exact shape of the conduction-band–energy profile and the interacting potential. If we model the impurity scattering in a 2D sample (x-y plane) by a δ-impurity interaction

$$V(x,y)=\gamma\delta(x-x_i)\delta(y-y_i) , \tag{B8}$$

then Eqs. (B5) can be written as

$$\frac{d^2C_n}{dx^2}+k_n^2C_n=\sum_m\tilde{\Gamma}_{nm}\delta(x-x_i)C_m , \tag{B9}$$

where $\tilde{\Gamma}_{nm}$ is given by Eq. (24) in the text. A scattering matrix relates the amplitudes of the modes incident on an obstacle from either direction of the amplitudes of the modes leaving the obstacle in either direction. In order to calculate the scattering matrix across a δ impurity, we first introduce the following new set of variables,

$$C_n^{+,-}(x)=\kappa_n\left[C_n\pm\frac{1}{ik_n}\frac{dC_n}{dx}\right] , \tag{B10}$$

which can easily be inverted to give

$$C_n=\frac{1}{2\kappa_n}(C_n^++C_n^-) , \tag{B11a}$$

$$\frac{dC_n}{dx}=\frac{ik_n}{2\kappa_n}(C_n^+-C_n^-) , \tag{B11b}$$

where, by definition,

$$\kappa_n = \frac{1}{2}\left[\frac{\hbar k_n}{m^*}\right]^{1/2} . \tag{B12}$$

The $C_n^{+,-}$ represent the amplitude of the current density in mode n traveling along the positive and negative x axis, respectively. Indeed, one can easily show using the definitions (B11a) and (B11b) that the current density can be written as follows,

$$J(x) = \sum_n J_n^+ - J_n^- , \tag{B13a}$$

where

$$J_n^+ = (C_n^+)^* C_n^+ \quad \text{and} \quad J_n^- = (C_n^-)^* C_n^- . \tag{B13b}$$

Assuming $E_c^x(x)$ to be piecewise continuous, integrating both sides of Eq. (B9) from $x_i - \varepsilon$ to $x_i + \varepsilon$ (ε being a small positive quantity), and taking into account the assumed continuity of the C_n's, we obtain

$$\left.\frac{dC_n}{dx}\right|_{x_i+\varepsilon} - \left.\frac{dC_n}{dx}\right|_{x_i-\varepsilon} = \sum_m \tilde{\Gamma}_{nm} C_m(x_i+\varepsilon) , \tag{B14}$$

which we rewrite as

$$\left.\frac{dC_n}{dx}\right|_{x_i+\varepsilon} = \left.\frac{dC_n}{dx}\right|_{x_i-\varepsilon} + \sum_m \tilde{\Gamma}_{nm} C_m(x_i+\varepsilon) . \tag{B15}$$

In Eq. (B14), we have assumed that all C_n's are continuous:

$$C_n(x_i+\varepsilon) = C_n(x_i) = C_n(x_i-\varepsilon) . \tag{B16}$$

Dividing Eq. (B15) by ik_n and adding the result to Eq. (B16), we get

$$\frac{1}{\kappa_n} C_n^+(x_i+\varepsilon) \equiv C_n(x_i+\varepsilon) + \frac{1}{ik_n}\left.\frac{dC_n}{dx}\right|_{x_i+\varepsilon} = \frac{1}{\kappa_n} C_n^+(x_i-\varepsilon) + \sum_m \frac{\tilde{\Gamma}_{nm}}{ik_n} C_m(x_i+\varepsilon) . \tag{B17}$$

Now, using Eqs. (B11a) and (B11b), we have

$$C_m(x_i+\varepsilon) = \frac{1}{2\kappa_m}[C_m^+(x_i+\varepsilon) + C_m^-(x_i+\varepsilon)] . \tag{B18}$$

Inserting this last result into Eq. (B17), we finally derive

$$C_n^+(x_i+\varepsilon) = C_n^+(x_i-\varepsilon) + \sum_m \frac{\tilde{\Gamma}_{nm}}{2i(k_m k_n)^{1/2}}[C_m^+(x_i+\varepsilon) + C_m^-(x_i+\varepsilon)] , \tag{B19}$$

or, equivalently,

$$C_n^+(x_i+\varepsilon) - \sum_m \frac{\tilde{\Gamma}_{nm}}{2i(k_m k_n)^{1/2}} C_n^+(x_i+\varepsilon) = C_n^+(x_i-\varepsilon) + \sum_m \frac{\tilde{\Gamma}_{nm}}{2i(k_m k_n)^{1/2}} C_m^-(x_i+\varepsilon) , \tag{B20}$$

valid for all modes n. The equations for the different modes can be written in a matrix form (which is done here for the case of two modes only for simplicity),

$$\begin{bmatrix} 1 - \dfrac{\tilde{\Gamma}_{11}}{2ik_1} & -\dfrac{\tilde{\Gamma}_{12}}{2i(k_1k_2)^{1/2}} \\ -\dfrac{\tilde{\Gamma}_{21}}{2i(k_1k_2)^{1/2}} & 1 - \dfrac{\tilde{\Gamma}_{22}}{2ik_2} \end{bmatrix} \begin{bmatrix} C_1^+(x_i+\varepsilon) \\ C_2^+(x_i+\varepsilon) \end{bmatrix} = \begin{bmatrix} 1 & 0 & \dfrac{\tilde{\Gamma}_{11}}{2ik_1} & \dfrac{\tilde{\Gamma}_{12}}{2i(k_1k_2)^{1/2}} \\ 0 & 1 & \dfrac{\tilde{\Gamma}_{21}}{2i(k_1k_2)^{1/2}} & \dfrac{\tilde{\Gamma}_{22}}{2ik_2} \end{bmatrix} \begin{bmatrix} C_1^+(x_i-\varepsilon) \\ C_2^+(x_i-\varepsilon) \\ C_1^-(x_i+\varepsilon) \\ C_2^-(x_i+\varepsilon) \end{bmatrix} , \tag{B21}$$

which we write more simply as

$$[I + (ia_{++})] \begin{bmatrix} C_1^+(x_i+\varepsilon) \\ C_2^+(x_i+\varepsilon) \end{bmatrix} = [I, \; -(ia_{++})] \begin{bmatrix} C_1^+(x_i-\varepsilon) \\ C_2^+(x_i-\varepsilon) \\ C_1^-(x_i+\varepsilon) \\ C_2^-(x_i+\varepsilon) \end{bmatrix} , \tag{B22}$$

I being the unit (2×2) matrix, and the matrix a_{++} is given by

$$a_{++} = \begin{bmatrix} \dfrac{\tilde{\Gamma}_{11}}{2k_1} & \dfrac{\tilde{\Gamma}_{12}}{2(k_1k_2)^{1/2}} \\ \dfrac{\tilde{\Gamma}_{21}}{2(k_1k_2)^{1/2}} & \dfrac{\tilde{\Gamma}_{22}}{2k_2} \end{bmatrix} . \tag{B23}$$

From Eq. (B22), we then deduce

$$\begin{bmatrix} C_1^+(x_i+\varepsilon) \\ C_2^+(x_i+\varepsilon) \end{bmatrix} = [I + ia_{++}]^{-1}[I, \ -ia_{++}] \begin{bmatrix} C_1^+(x_i-\varepsilon) \\ C_2^+(x_i-\varepsilon) \\ C_1^-(x_i+\varepsilon) \\ C_2^-(x_i+\varepsilon) \end{bmatrix}, \tag{B24}$$

or, equivalently,

$$\begin{bmatrix} C_1^+(x_i+\varepsilon) \\ C_2^+(x_i+\varepsilon) \end{bmatrix} = [(I + ia_{++})^{-1}, \ -(I + ia_{++})^{-1}(ia_{++})] \begin{bmatrix} C_1^+(x_i-\varepsilon) \\ C_2^+(x_i-\varepsilon) \\ C_1^-(x_i+\varepsilon) \\ C_2^-(x_i+\varepsilon) \end{bmatrix}. \tag{B25}$$

Similarly, dividing Eq. (B15) by ik_n, subtracting the obtained result from Eq. (B16), and following a similar derivation, we get

$$\begin{bmatrix} C_1^-(x_i-\varepsilon) \\ C_2^-(x_i-\varepsilon) \end{bmatrix} = [-(I + ia_{++})^{-1}(ia_{++}), \ (I + ia_{++})^{-1}] \begin{bmatrix} C_1^+(x_i-\varepsilon) \\ C_2^+(x_i-\varepsilon) \\ C_1^-(x_i+\varepsilon) \\ C_2^-(x_i+\varepsilon) \end{bmatrix}. \tag{B26}$$

Grouping the results (B25) and (B26), we obtain the final relation

$$\begin{bmatrix} C_1^-(x_i-\varepsilon) \\ C_2^-(x_i-\varepsilon) \\ C_1^+(x_i+\varepsilon) \\ C_2^+(x_i+\varepsilon) \end{bmatrix} = \begin{bmatrix} -(I + ia_{++})^{-1}(ia_{++}) & (I + ia_{++})^{-1} \\ (I + ia_{++})^{-1} & -(I + ia_{++})^{-1}(ia_{++}) \end{bmatrix} \begin{bmatrix} C_1^+(x_i-\varepsilon) \\ C_2^+(x_i-\varepsilon) \\ C_1^-(x_i+\varepsilon) \\ C_2^-(x_i+\varepsilon) \end{bmatrix}, \tag{B27}$$

where the square matrix is the required scattering matrix [see Eq. (22) in the text].

For the general case of M modes, we can easily generalize the 2×2 matrix given in Eq. (B23). The general expression of the matrix elements of a_{++} can be written as

$$(a_{++})_{mn} = \frac{1}{2} \frac{\tilde{\Gamma}_{mn}}{(k_n k_m)^{1/2}}. \tag{B28}$$

---

*Permanent address: Scientific Research Associates, Inc., Glastonbury, CT 06033.

[1]E. Abrahams, P. W. Anderson, D. C. Licciardello, and T. V. Ramakrishnan, Phys. Rev. Lett. **42**, 673 (1979).

[2]S. Washburn and R. A. Webb, Adv. Phys. **35**, 375 (1986), and references therein.

[3]K. Ishibashi, K. Nagata, K. Gamo, S. Namba, S. Ishia, K. Murase, M. Kawabe, and Y. Aoyagi, Solid State Commun. **61**, 385 (1987).

[4]W. J. Skoçpol, P. M. Mankiewich, R. E. Howard, L. D. Jackel, D. M. Tennant, and A. D. Stone, Phys. Rev. Lett. **56**, 2865 (1986).

[5]H. Van Houlen, B. J. Van Wess, M. G. J. Heijman, and J. P. Andre, Appl. Phys. Lett. **49**, 1781 (1986).

[6]S. Y. Chou, D. A. Antoniadis, H. I. Smith, and M. A. Kastner, Solid State Commun. **61**, 571 (1987).

[7]G. P. Whittington, P. C. Main, L. Eaves, R. P. Taylor, S. Thoms, S. P. Beaumont, and C. P. W. Wilkinson, Superlattices Microstruct. (Berlin) **2**, 385 (1986).

[8]S. C. Feng, P. A. Lee, and A. D. Stone, Phys. Rev. Lett. **56**, 1960 (1986); **56**, 2772(E) (1986).

[9]P. A. Lee, A. D. Stone, and H. Fukuyama, Phys. Rev. B **35**, 1039 (1987).

[10]B. L. Alt'shuler, Pis'ma Zh. Eskp. Teor. Fiz. **41**, 530 (1985) [JETP Lett. **41**, 648 (1985)].

[11]Y. Imry, Europhys. Lett. **1**, 249 (1986).

[12]P. A. Lee, Physica A **140**, 169 (1986).

[13]A. D. Stone, Phys. Rev. Lett. **54**, 2692 (1985).

[14]P. W. Anderson, Phys. Rev. **109**, 1492 (1958).

[15]N. Giordano, Phys. Rev. B **36**, 4190 (1987).

[16]J. Sak and B. Kramer, Phys. Rev. B **24**, 1761 (1981).

[17]A. Fuchs and G. Mahler, Solid State Commun. **55**, 1035 (1985).

[18]C. J. Lambert and M. F. Thorpe, Phys. Rev. B **27**, 715 (1983).

[19]P. Eordos and R. C. Henderson, Adv. Phys. **31**, 65 (1982).

[20]S. Datta, M. R. Melloch, S. Bandyopadhyay, R. Noren, M. Vaziri, M. Miller, and R. Reifenberger, Phys. Rev. Lett. **55**, 2344 (1985); G. Timp, A. M. Chang, P. M. Mankiewich, R. Behringer, J. E. Cunnigham, T. Y. Chang, and R. E. Howard, *ibid.* **59**, 732 (1987).

[21]R. Landauer, IBM J. Res. Dev. **1**, 223 (1957); Philos. Mag. **21**, 863 (1970).

[22]This is the two-probe multichannel Landauer formula which we use in the most of our calculations. For near-ballistic

transport we also consider the four-probe formula [Eq. (26)].
[23]P. A. Lee, Phys. Rev. Lett. **42**, 1492 (1979).
[24]A similar technique for combining scattering matrices has been used recently to characterize wave propagation in microstrip step discontinuities, T. S. Chu and T. Itoh, IEEE Trans. Microwave Theor. Technol. **MTT-34**, 280 (1986); see also R. Redheffer, J. Math. Phys. **41**, 1 (1962).
[25]B. Shapiro, Phys. Rev. B **35**, 8256 (1987).
[26]P. W. Anderson, Phys. Rev. B **23**, 4828 (1981).
[27]L. I. Schiff, *Quantum Mechanics*, 3rd ed. (McGraw-Hill, New York, 1968), p. 308.
[28]S. Datta, M. Cahay, and M. McLennan, Phys. Rev. B **36**, 5655 (1987): in this paper there is a small misprint in Eq. (8) which should be replaced by Eq. (17) of this paper.
[29]D. J. Thouless, Phys. Rev. Lett. **39**, 1167 (1977).
[30]G. Bergman, Phys. Rev. B **28**, 2914 (1983).
[31]P. W. Anderson, Phys. Rev. B **23**, 4828 (1981); a somewhat different multichannel Landauer formula has been given by M. Büttiker, Y. Imry, R. Landauer, and S. Pinhas, Phys. Rev. B **31**, 6207 (1985), and M. Ya. Azbel, J. Phys. C **14**, L225 (1981).
[32]M. Büttiker, Phys. Rev. B **35**, 4123 (1987).
[33]For model B, the semiclassical conductance of the samples (Fig. 9) is $\sim 5e^2/h$ after crossing 2×10^3 impurities; we thus deduce from Eq. (19) that $\Lambda_{el}\sim 400$.